HARDWARE-IN-THE-LOOP SIMULATION FOR SMALL-SCALE HELICOPTER CONTROL SYSTEMS ASSESSMENT

Giulia Bertolani
University of Bologna
Forlì, Italy

Daniele Fattizzo
University of Bologna
Forlì, Italy

Francesco Mazzeo
University of Modena and Reggio Emilia, Italy

Fabrizio Giulietti
University of Bologna
Forlì, Italy

Emanuele Luigi de Angelis
University of Bologna
Forlì, Italy

ABSTRACT

This paper proposed a methodology for validating small-scale unmanned helicopter flight control systems by means of Hardware-In-the-Loop (HIL) simulations. To this aim, two control architectures are compared: a standard Proportional-Integral-Derivative (PID) controller and a Sliding Mode Control (SMC) technique combined with PID. The HIL setup employs a Pixhawk® 6x Flight Management Unit (FMU) and Matlab/Simulink® for real-time dynamic simulation, allowing the implementation of control algorithms in a near-realistic conditions. Results for two different maneuvers, the bob-up/bob-down and the circular trajectory tracking demonstrates suitability of the proposed approach, by highlighting the relevance of computational requirements in the flight hardware design and selection phases. In this respect, HIL simulations represents a valuable tool for the development and refinement of UAV control systems, while improving performance and reliability.

1. INTRODUCTION

The use of Software and Hardware-in-the-Loop (SIL, HIL) techniques plays a relevant role in the design and prototyping process of flight control systems. As a matter of fact, the possibility to test control systems in a Real-Time environment, which includes the flight software and hardware, allows to preliminary validate the control architecture without the cost (and risks) associated to an experimental flight campaign. This become crucial, in the field of Unmanned Aerial Vehicles (UAVs); the increasing demand for agile, efficient, and highly-automated platforms within a wide range of applications (surveillance, search and rescue, and environmental monitoring), drives to the need of a fast and reliable design and prototyping process of control algorithms (Refs. 1,2).

Among the several UAV configurations, small-scale remotely-piloted helicopters have become of interest within the Unmanned System community. With respect to multi-rotors platforms, well recognized for their mechanical simplicity and maneuverability, conventional helicopters present an higher cargo capabilities (higher thrust-to-weight ratio) and a wider flight envelope. Also, enhanced emergency-management capabilities represent a valuable feature (Ref. 3). The main drawback of the helicopter configuration, is represented by its natural instability and its highly non-linear dynamic behavior. Thus, robust attitude control strategies shall be foreseen to ensure stable flight conditions and accurate trajectory tracking (Ref. 4).

Besides the continuous effort in the research and exploration of new control approaches, an important challenge is the smart integration between the designed control algorithms and the real on-board hardware. In this respect, a crucial task is the consistency between the required computational burden and the flight hardware's capabilities. To this aim, the Hardware-in-the-Loop (HIL) technique is a powerful methodology for validating and comparing different implementations of UAVs control architectures. The HIL simulation, thanks to the Real-Time dialog between 1) the actual flight processor and 2) mathematical models representing aircraft, systems dynamics, and external environment, allows for a comprehensive testing and validation of control algorithms under realistic operating conditions (Refs. 5–8), without the risk of damages for the aircraft or incurring substantial costs associated with traditional flight testing.

A wide use of HIL simulations for UAVs applications can be found within the scientific literature. Prabowo et al. (Ref. 9) implemented a real-time HIL system to support vision-based controller hardware of image processing module and visual-based controller module for a fixed-wing UAV. In (Ref. 10) a decentralized approach to multiplatform HIL simulation of UAV swarm is presented. Omar (Ref. 5) developed a HIL simulation platform for a quadrotor with a suspended load system using Gazebo. Sun et al. (Ref. 11) designed a complete HIL testbed for the simulation and testing of a tail-sitter vehicle and then examined it with the flight tests. A 3 Degrees-Of-Freedom (DOF) HIL test platform to test controls for multirotor UAVs was designed and presented in (Ref. 7), while in (Ref. 8) a HIL demonstrator is developed to validate fault-tolerant controllers for a hybrid UAV. Yu et al. (Ref. 12) employed the HIL to verify the performance and software design of the control scheme for a tiltrotor UAV. With respect to small-scale unmanned helicopters, Khaligh et al. (Ref. 13) designed a HIL testbed to tune controller gains for a small helicopter platform, whereas Pizetta et al. (Ref. 6) implemented a HIL platform capable of simulating different mathematical models and control strategies for commercial miniature helicopters. In (Ref. 14) the HIL is used to simulate several flight tests for UAV helicopters. Also, HIL simulation technique is also used to compare different control techniques, as in (Refs. 15–18) where multiple control techniques are implemented to evaluate their performance and robustness for UAV applications.

Different architectures involving flight HW and SW and the simulated environments can be considered. The basic structure, namely the Processor-in-the-Loop, PIL, is represented by the actual onboard computer where flight control algorithms are implemented in order to close the feedback loop with the simulated environment made of system dynamics, sensors, and actuators. In the present paper, a HIL simulation technique is developed and implemented according to the PIL architecture with the purpose to assess the performance of small-scale helicopter control algorithms. To this aim, two different control architectures are considered: i) the classical Proportional-Integral-Derivative (PID) controller, and ii) a Sliding Mode Control (SMC) technique, combined with classical Proportional-Integral-Derivative controllers. The selected Flight Management Unit (FMU) representing flight hardware is the Pixhawk® 6x coupled with the PX4 flight stack firmware. The FMU is interfaced with the computer through a serial connection. The simulation environment employed for this work is Matlab/SImulink®, with which the control algorithms are generated and updated on the FMU.

The rest of paper is organized as follows: Section 2 gives an overview of the mathematical model used to simulate the small-scale helicopter dynamics; Section 3 describes the control systems architectures; the Hardware-In-the-Loop set-up is detailed in Section 4; Section 5 shows the HIL simulation results; conclusions are discussed in Section 6.

2. SMALL-SCALE HELICOPTER MATHEMATICAL MODEL

2.1. Rigid body dynamics

The mathematical model of the small-scale helicopter is briefly presented in this section. It is based on the work of Talbot (Ref. 19) and it has been yet presented by the authors in some of their works (Refs. 3, 20).

The model is for a standard helicopter configuration featuring a single main rotor and a tail rotor. Each segment of the small-scale helicopter, including the main rotor, tail rotor, and fuselage, was independently modeled. The cumulative forces and moments exerted at the helicopter center of gravity were determined by summing the contributions from all individual components, along with gravitational forces. The model assumes a flat, non-rotating Earth with a constant gravitational field. The helicopter mass and its distribution are assumed to be constant for the duration of the study.

Helicopter dynamics is described according to the Newton-Euler equations of motion:

$$\dot{\mathbf{v}} = -\omega \times \mathbf{v} + \mathbf{F^e}/\mathbf{m} \tag{1}$$

$$\dot{\omega} = J^{-1}\left[-\omega \times (J\,\omega) + \mathbf{M^e}\right] \tag{2}$$

where ω is the angular velocity, $\mathbf{v}$ is the linear body velocity, $\mathbf{F^e}$ and $\mathbf{M^e}$ are the external forces and moments vectors, J is the inertia tensor about CG and m is the total mass of the helicopter. The external forces acting on the small-scale helicopter include gravitational force, $F^{(g)}$, and aerodynamic forces $F^{(a)}$. The gravitational force vector is given by:

$$F^{(g)} = \Pi_{be} \begin{bmatrix} 0 \\ 0 \\ m\,g \end{bmatrix} = m\,g \begin{bmatrix} -\sin\theta \\ \sin\phi\,\cos\theta \\ \cos\phi\,\cos\theta \end{bmatrix} \tag{3}$$

where g is the gravitational acceleration and Π_{be} is the rotation matrix between inertial and body frame of reference. The aerodynamic forces, $F^{(a)} = [X,Y,Z]^T$, and moments, $M^{(a)} = [L,M,N]^T$, are characterized based on the model detailed in (Ref. 19). These contributions originate from the main rotor, tail rotor, and fuselage of the small-scale helicopter. Air parameters are computed using the International Standard Atmosphere (ISA) model as a function of the rotorcraft's altitude (Ref. 21).

The fuselage is modeled as a virtual flat plate drag source with three dimensions, as outlined in (Ref. 22). The forces and moments acting on the fuselage are computed as functions of the angle of attack and the sideslip angle.

2.2. Main rotor model

The main rotor model is based on the following assumptions: (a) the rotor blades are considered rigid in both bending and torsion; (b) small flapping angles are assumed, and the simple strip theory is applied (Ref. 23); (c) blade flow stall effects are neglected; (d) the flapping motion of the main rotor blades is represented by the first harmonic terms with time-dependent coefficients, described by:

$$\beta(t) = a_0(t) - a_1(t)\,\cos\xi - b_1(t)\,\sin\xi \tag{4}$$

where $a_0(t)$ is a preset constant and ξ is blade azimuth. $a_1(t)$ and $b_1(t)$ correspond to the longitudinal and lateral tilt of the rotor tip-path plane at time t, respectively. Under these assumptions, the blade element theory is applied, and the forces on the blades are analytically integrated over the rotor radius. Ref. (Ref. 19) contains comprehensive formulas for computing forces and moments. For modeling the inflow, the Pitt-Peters dynamic inflow model (Ref. 24) is employed, assuming it to be uniform.

2.3. Tail rotor model

The tail rotor is modeled following the approach described in (Ref. 19), with the assumption of no cyclic pitch control. Given that the flapping frequency of the tail rotor is generally much higher than that of the main rotor, the dynamics of the tail rotor tip-path plane is neglected. As a result, the forces, moments, and flapping angles are considered to be in steady-state.

3. CONTROL SYSTEMS ARCHITECTURE

The overall helicopter control system is made of two feedback loops according to the nested loop architecture, as shown in Figure 1. The inner control loop has to deal with attitude stabilisation, whereas the outer control loop is a speed autopilot. The input for the outer loop is the reference velocity signal provided by the external pilot , whereas the output is the reference roll and pitch attitude for the inner control loop. With respect to the yaw axis, the external pilot directly commands a reference yaw rate, whereas the altitude hold controller gets the reference vertical speed also commanded by external pilot.

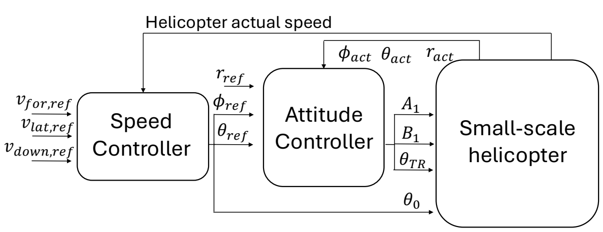

Figure 1. Small-scale helicopter control architecture

Two different control technique are developed and validated by means of HIL simulations. The proposed techniques share the same inner loop, and they show a different the outer loop: one hand, classical PID controllers are implemented; on the other hand, the sliding mode control technique is provided. In the following sections, a detailed description of the control architecture is provided.

3.1. Attitude controller

PID approach is the basis of the inner control loop for the attitude of the UAV on the distinct axes of roll, pitch, and yaw. It consists of a cascade control system (Ref. 25). The external loop places the set point for the inner one. On lateral and longitudinal axes, the control system has the same structure, while on the yaw axis only the yawrate r is controlled, as depicted in Figure 2. The outer loop addresses the roll angle ϕ and pitch angle θ with a proportional gain, while the inner loop uses a proportional integral technique to handle the angular rates p (rollrate), q (pitchrate) and r (yawrate).

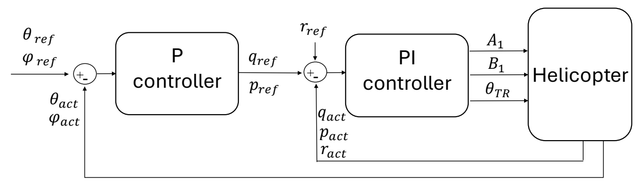

Figure 2. Small-scale helicopter PID attitude control scheme

3.2. Altitude hold controller

Altitude hold controller is part of the speed hold control loop, but it is a PID cascade control scheme and it directly generates the small-scale helicopter main rotor collective command. Vertical speed v_d and acceleration a_d are controlled. The pilot input is a reference vertical velocity, that is integrated. On the vertical acceleration there is a derivative action, as reported in the scheme in Figure 3.

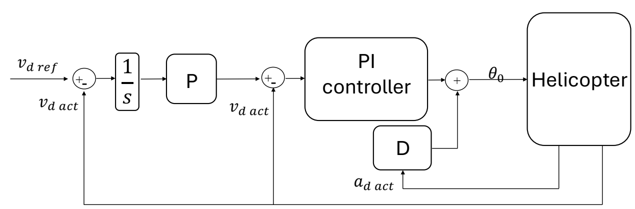

Figure 3. Small-scale helicopter PID altitude hold control scheme

3.3 Speed hold controller

Both the speed hold control schemes are described in this section.

PID speed hold controller The speed-hold control scheme is a classical Proportional-Integral controller acting on the forward and lateral velocities evaluated in the Local-Vertical axes frame, that is centered in the vehicle Center of Gravity (CG), parallel to North-East-Down axes X_N and Y_E, but aligned with the helicopter heading ψ. The outputs of the PID controller are the desired forward and lateral accelerations, that are converted in reference angles θ_{ref} and ϕ_{ref} for the attitude controller as follows:

$$\phi_{ref} = \arctan \frac{a_l \cos\theta_{ref}}{g}$$
$$\theta_{ref} = -\arctan \frac{a_f}{g} \tag{5}$$

where g is again the gravity acceleration, a_f and a_l are the forward and the lateral accelerations in the Local-Vertical frame, respectively. Control scheme is reported in Figure 4.

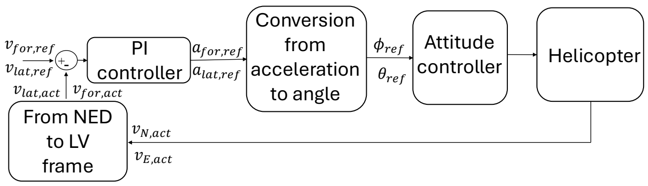

Figure 4. Small-scale helicopter PID speed hold control scheme

SMC speed hold controller The sliding mode technique is used and tested in HIL simulation as an alternative speed hold control scheme on longitudinal and lateral axes. The scheme is given in Figure 5. As for PID speed hold controller, reference signal for forward and lateral velocities are in the Local-Vertical frame. The outputs are the reference attitude angles for the inner control loop.

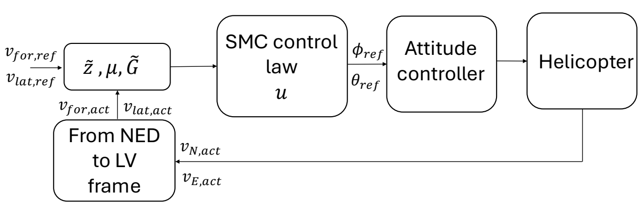

Figure 5. Small-scale helicopter SMC speed hold control scheme

This control scheme has been yet presented by some of the authors in (Ref. 26). SMC control theory overview is detailed in (Ref. 27) and here briefly summarized.

The following sliding surfaces μ are chosen:

$$\mu = \begin{bmatrix} v_l + \lambda_l \int_0^t \left(v_l - v_{l,ref}\right) d\tau \\ v_f + \lambda_f \int_0^t \left(v_f - v_{f,ref}\right) d\tau \end{bmatrix} \tag{6}$$

where λ_l, λ_f are the inverse time period. Such sliding surfaces describe the desired forward and lateral speed dynamics that the UAV has to track. $\tilde{z}$ is the augmented state vector $\tilde{z} = [z_e\ z]'$, where $z = [v_l\ v_f]'$ is the outer loop state and z_e the tracking error. $\dot{z}_e = (w - q)$ with $w = [v_l\ v_f]'$ and $q = [v_{l,ref}\ v_{f,ref}]'$. $\tilde{G} = \begin{bmatrix} 0_{2x2} \\ G \end{bmatrix}$ is the matrix that represents the forward and lateral accelerations, where G is:

$$\begin{bmatrix} a_f \\ a_l \end{bmatrix} = G \begin{bmatrix} \Delta\theta \\ \Delta\phi \end{bmatrix}$$

$$G = \begin{bmatrix} -g & g \tan\theta \tan\phi \\ 0 & g/\cos\theta \end{bmatrix}$$

The control law is given by:

$$u = -(R\tilde{G})^{-1}((R\tilde{F} - 0.5R)\tilde{z} + (0.5R_3 - R\tilde{T}_0)q - R_3\dot{q} + \rho_0 sat(\mu/\varepsilon_0)) \tag{7}$$

where $R = [R_1 R_2]'$, $\rho_0 = diag(\rho_{01}\ \rho_{02})$, $sat(\mu/\varepsilon_0)) = [sat(\mu_1/\varepsilon_0)\ sat(\mu_2/\varepsilon_0)]'$ and $\tilde{F} = \begin{bmatrix} 0_{2x2} & I_2 \\ 0_{2x2} & 0_{2x2} \end{bmatrix}$. $R_1 = \begin{bmatrix} \lambda_l & 0 \\ 0 & \lambda_f \end{bmatrix}$, $R_2 = \begin{bmatrix} 1 & 0 \\ 0 & 1 \end{bmatrix}$, $R_3 = \begin{bmatrix} -1 & 0 \\ 0 & -1 \end{bmatrix}$ and $\tilde{T}_0 = \begin{bmatrix} I_2 \\ 0_{2x2} \end{bmatrix}$, where I_2 is a $2x2$ identity matrix.

4. HARDWARE-IN-THE-LOOP SETUP

Hardware in the loop (HIL) is a simulation technique where two main subsystems communicate and collaborate. A host computer is used to simulate the dynamics of the vehicle and the atmospheric environment, while external hardware is involved in the real-time calculation of the control action on the system. This hardware is generally the same installed on the real UAV. Different levels of hardware-software equilibrium can be set for a HIL simulation: often physical actuators can be included in the loop. For a small-scale helicopter, as for the present study, no actuator dynamics and neither physical actuators are considered. Hardware in the loop is an important tool for validating the control system architecture and studying the agreement between the computational burden required by the controller and the hardware capabilities. This technique represents a crucial step between the purely numerical simulation, where a single model simulates both the dynamics and the control system, and the flight test with real platforms. The hardware adopted in the present work is the Pixhawk® 6X controller, coupled with the PX4 flight stack firmware for HIL testing. The flight controller is interfaced with the host computer through a serial connection and the PC runs Matlab/Simulink® software to simulate the helicopter dynamics. QGround Control is the ground station, which is used to manage the communication between the host and the hardware. The control algorithms are generated from Simulink® using the *Matlab embedded coder* and uploaded on the Pixhawk® controller. The simulation is performed in the "Monitor and Tune" mode, which consists of two Matlab® sessions: one for the plant simulation, and the other one, in "External Mode", where the Simulink® model, uploaded to the hardware, receives back the signals read and processed by Pixhawk®. The procedure is described in deep detail in (Ref. 28). The scheme of the HIL components and interfaces is depicted in Figure 6.

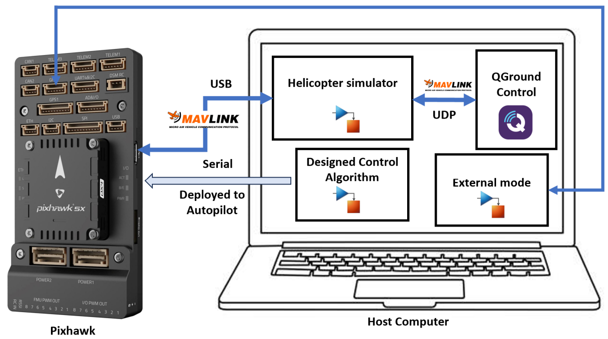

Figure 6. HIL components and communication scheme

5. HIL SIMULATION RESULTS

Both the control architectures presented in previous sections are tested by means of HIL simulations. The small-scale helicopter model adopted as dynamic model for the simulations is briefly detailed in Section 2. Data for this UAV are reported in Table 1. These parameters are those of the SAB Goblin Black Thunder 700 small-scale remotely piloted helicopter.

Two different maneuvers have been considered to test the performance of the developed controllers uploaded on the Pixhawk® 6x.

Control system architectures are tested by means of two different maneuvers: 1) the bob-up/bob-down maneuver, that consists in a sequence of longitudinal and vertical steps; 2) circular maneuver, in which the UAV is asked to describe a circle regulating the longitudinal and yawrate speeds. The military standard (Ref. 29) that has been created guided the choice of the selected maneuvers. The first maneuver is a straightforward combination of segments that are vertical and horizontal. The hovering condition is the initial point of the bob-up/bob-down. The UAV is then asked to track a reference speed of 5 m/s for 20 seconds, while maintaining a constant altitude, and it is then decelerated to 0 m/s. After this, the UAV has to follow a descent speed of 2 m/s for 10 seconds and then it is again decelerated to hovering. The longitudinal reference speed is again 5 m/s for 20 seconds and, from hovering, finally a vertical climbing speed of 2 m/s is asked to be tracked by the controller for 10 seconds. Heading angle and lateral velocity references are zero for all the maneuver time. The second manuever is the circular one. In this case, the speed control system has to track a reference longitudinal speed while following a reference yawrate r on the yaw axis.

Results for the PID-based velocity controller and the sliding mode controller are reported in what follows.

5.1 Test of PID controller

Bob-up/bob-down maneuver Figures 7 and 8 show the main helicopter variables during the bob-up/bob-down maneuver when the PID speed controller is adopted. The reference velocity is quite well tracked by the system along the longitudinal and vertical directions. A certain difference can be observed between the first and the second steps on V_f. An overshooting is reported in the first case, while the system shows to be slower in the second case. The nonlinearity of the small-scale helicopter system is highlighted by the excitation on V_f when a vertical velocity is commanded. Looking at the lateral variables, good control is obtained on the velocity which is kept near the zero correcting the roll angle. A good control is also obtained for the yaw angle which is kept almost constant.

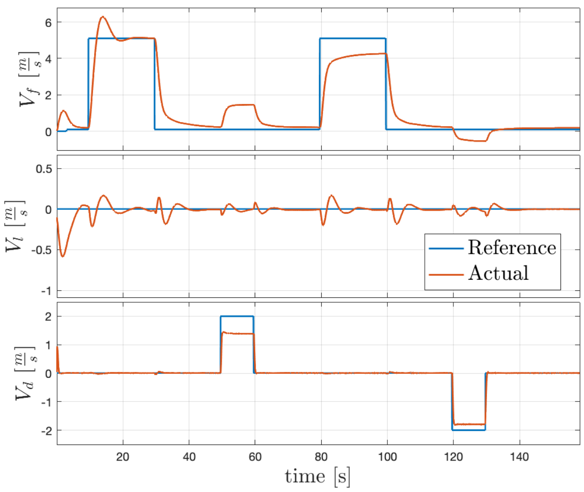

Figure 7. Reference vs Actual velocities during bob-up/bob-down maneuver - PID control architecture

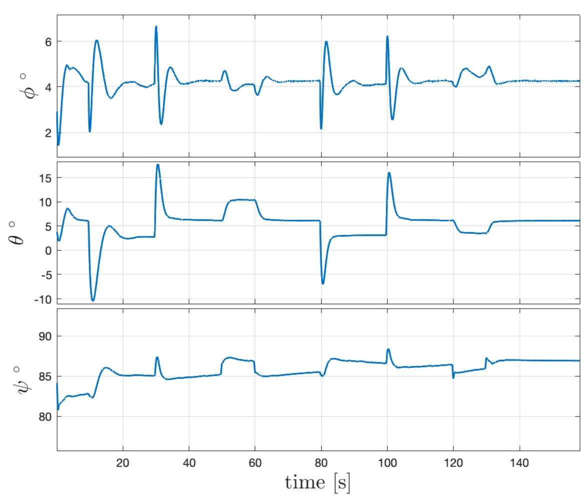

Figure 8. Attitude angles during bob-up/bob-down maneuver - PID control architecture

Circular maneuver In this maneuver the theoretical diameter of the circle is given by: $D = 2V_f/r = 21.4$ m. Figure 9 reports the reference and the actual velocities during the maneuver, while the attitude is showed in Figure 10 and the obtained trajectory is given in Figure 11. A good tracking of the advancing velocity and the yawrate is here shown. The UAV is capable to track a circle. The error between the theoretical and actual turn diameter is around 1 m, e.i. less than 5%.

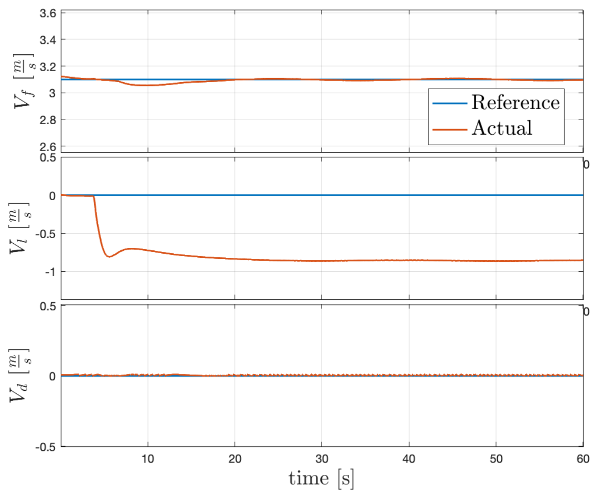

Figure 9. Reference vs Actual velocities during circular maneuver - PID control architecture

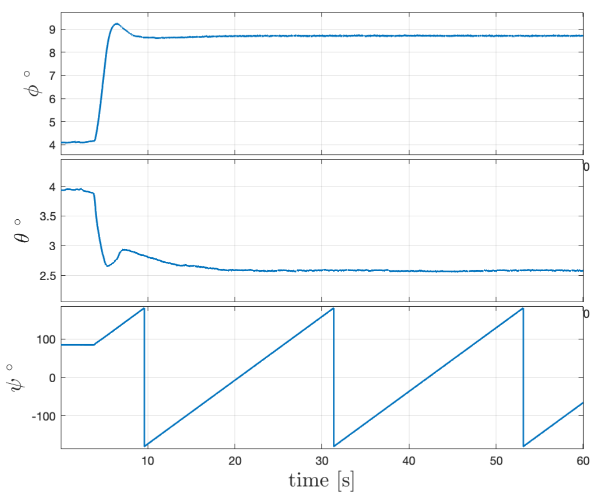

Figure 10. Attitude angles during circular maneuver - PID control architecture

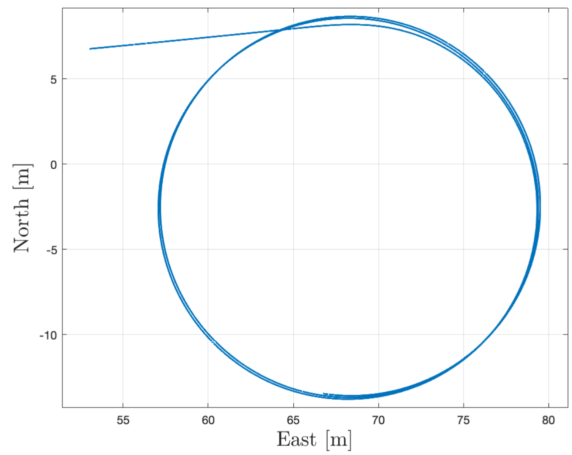

Figure 11. Circular tracking on X and Y axes - PID control architecture

5.2 Test of SMC controller

Bob-up/bob-down maneuver The same simualtions presented for PID speed control architecture have been conducted implementing a speed controller based on the sliding mode technique. The results for the bob-up bob-down maneuver are reported in Figures 12-13. It is possible to notice that the sliding mode control properly follows the reference velocities. Better tracking capabilities are obtained w.r.t. the PID case, as discussed in Section 5.3. From these plots it is possible to notice that the SMC produces a high frequency command action, the so called "chattering", which is typical of this control technique and might be more effectively avoided by refining the tuning of the boundaries ε_0 of the controller.

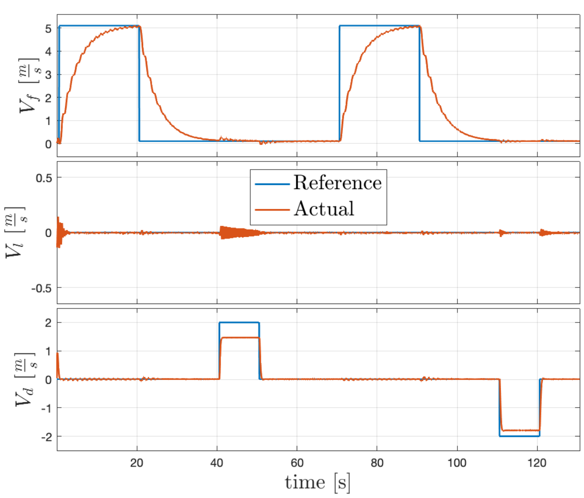

Figure 12. Reference vs Actual velocities during bob-up/bob-down maneuver - SMC control architecture

Circular maneuver For the circular maneuver, results for SMC speed controller and attitude are reported in Figures 14-15. The covered trajectory is showed in Figure 16 Again, the controller properly performs the maneuver, even if more evident oscillations result in the actual forward velocity.

5.3 Performance assessment

Bob-up/bob-down maneuver In Figure 17 the normal distributions of forward speed reference tracking errors for both the PID and SMC controller are given when the helicopter is simulated to perform a bob-up/bob-down maneuver. Both controllers show strong ability to track the desired forward speed, with a mean error of about zero. In Figure 18 the

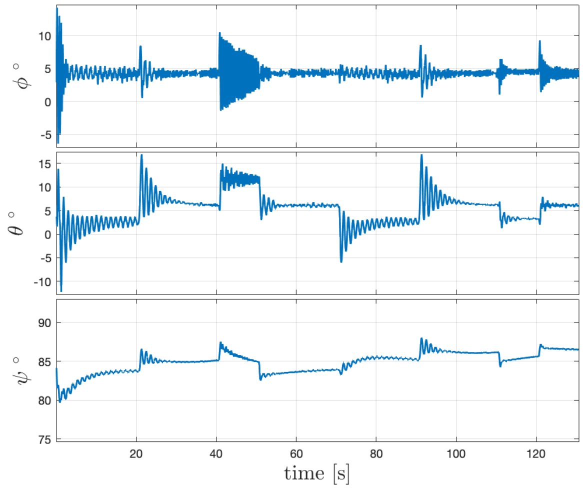

Figure 13. Attitude angles during bob-up/bob-down maneuver - SMC control architecture

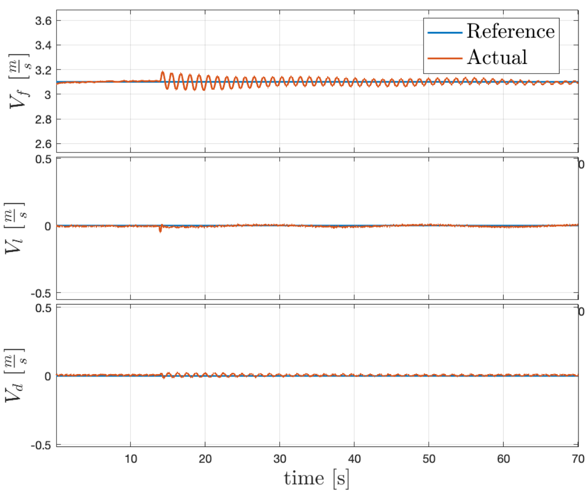

Figure 14. Reference vs Actual velocities during circular maneuver - SMC control architecture

normal distribution is reported for the lateral speed reference tracking errors of PID and SMC controllers.

Circular maneuver In Figures 19,20 the normal distributions of forward and lateral velocities reference tracking errors for both the PID and SMC controller are given during the circular maneuver. In this condition, the sliding mode controller exhibits better tracking performances, especially on the lateral axis.

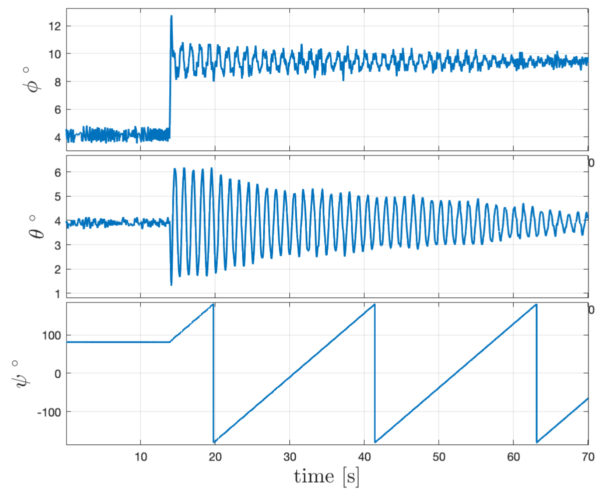

Figure 15. Attitude angles during circular maneuver - SMC control architecture

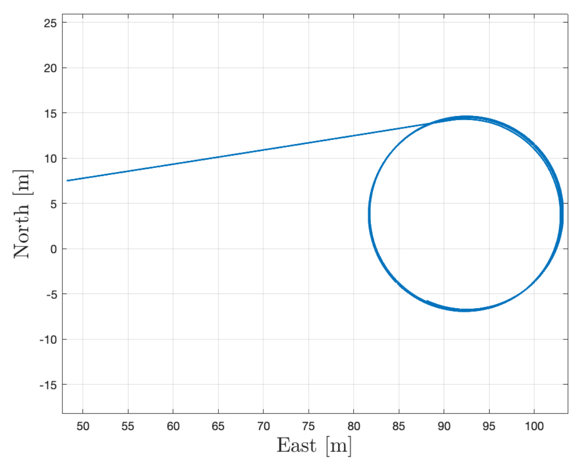

Figure 16. Circular tracking on X and Y axes - SMC control architecture

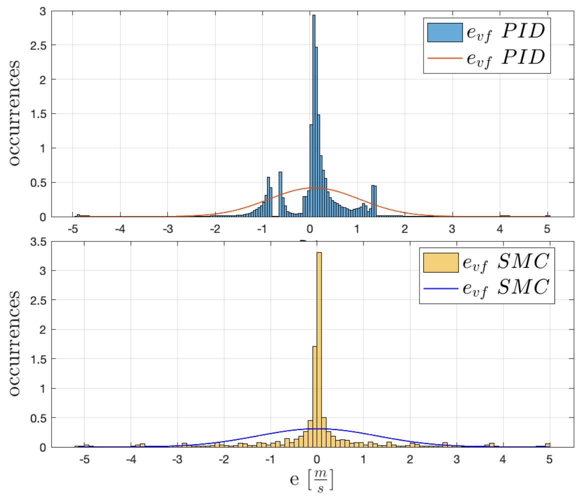

Figure 17. Forward speed error Gaussian distribution during bob-up/bob-down maneuver

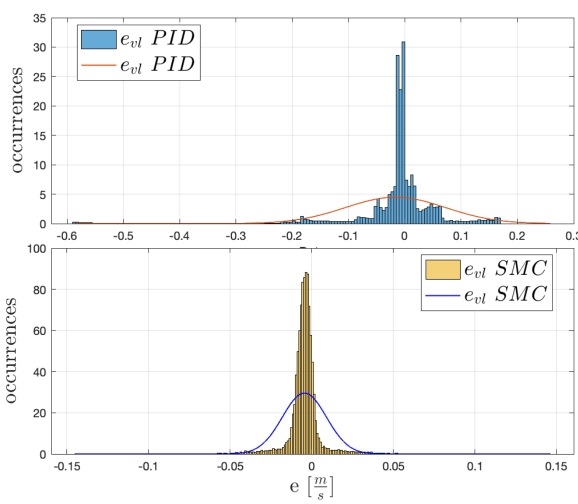

Figure 18. Lateral speed error Gaussian distribution during bob-up/bob-down maneuver

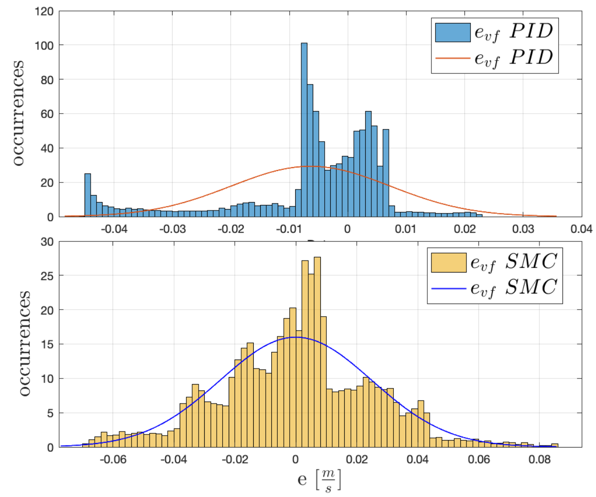

Figure 19. Forward speed error Gaussian distribution during circular maneuver

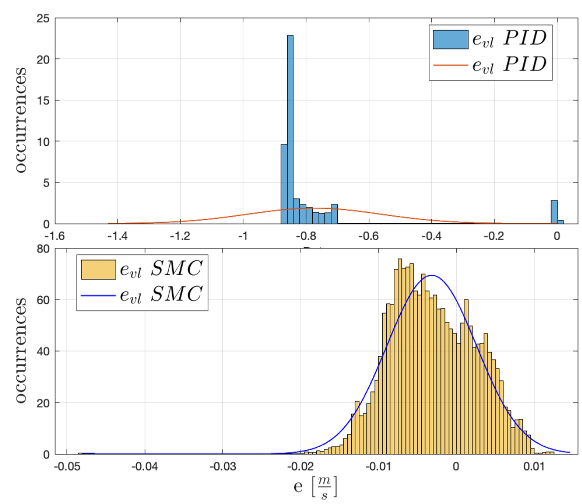

Figure 20. Lateral speed error Gaussian distribution during circular maneuver

6. CONCLUSIONS

This study addressed an Hardware-In-the-Loop (HIL) simulation architecture for small-scale helicopter control systems' performance assessment. By comparing two control techniques, a classical Proportional-Integral-Derivative (PID) controller and a Sliding Mode Controller combined with PID controller, the relevance of HIL simulations in evaluating and refining UAV control strategies has been demonstrated.

The HIL setup integrates the Pixhawk® 6x Flight Management Unit (FMU) with the PX4 flight stack firmware, interfaced with Matlab/Simulink® for dynamic simulation, proved to be an effective platform for real-time testing, enabling a comprehensive testing procedure for helicopter control system in a safe and cost-effective method, avoiding the risks associated with physical flight testing.

Results demonstrate a satisfactory performance for both the control schemes. A proper tracking of reference speeds has also been obtained for different maneuvers. The SMC technique showed superior performance in terms of tracking accuracy and robustness, especially during the more demanding circular maneuver. The SMC controller enhanced tracking ability, reveals its improved capability to handle nonlinearities and external disturbances.

Moreover, the study underscored the importance of considering the computational burden imposed by advanced control algorithms on flight hardware. The HIL simulation facilitated an in-depth analysis of the interplay between control strategies and hardware capabilities, ensuring that the implemented algorithms are both effective and feasible for real-world applications.

Overall, this research confirms the significant potential of HIL simulations in the iterative design and validation process of UAV control systems. By enabling early detection of design faults and providing a robust testing environment, HIL simulations can substantially accelerate the development cycle and enhance the reliability of small-scale helicopter control systems.

Future work will focus on further refinement of the control algorithms and expansion of the HIL framework to include additional sensors and actuators. In addition, some experimental tests will be conducted to effectively validate the proposed control architectures. This will provide a more comprehensive assessment platform for next-generation UAVs.

Author contact:
Giulia Bertolani giulia.bertolani2@unibo.it
Daniele Fattizzo daniele.fattizzo2@unibo.it
Francesco Mazzeo francesco.mazzeo@unimore.it
Fabrizio Giulietti fabrizio.giulietti@unibo.it
Emanuele Luigi de Angelis emanuele.deangelis4@unibo.it

ACKNOWLEDGMENTS

This study was carried out within the MOST - Sustainable Mobility National Research Center and received funding from the European Union Next-GenerationEU (PIANO NAZIONALE DI RIPRESA E RESILIENZA (PNRR) - MISSIONE 4 COMPONENTE 2, INVESTIMENTO 1.4 - D.D. 1033 17/06/2022, CN00000023). This manuscript reflects only the authors' views and opinions, neither the European Union nor the European Commission can be considered responsible for them.

REFERENCES

1. Faiyaz Ahmed, J. C. Mohanta, Anupam Keshari, and Pankaj Singh Yadav. Recent advances in unmanned aerial vehicles: A review. 47(7):7963–7984.

2. Khaled Telli, Okba Kraa, Yassine Himeur, Abdelmalik Ouamane, Mohamed Boumehraz, Shadi Atalla, and Wathiq Mansoor. A comprehensive review of recent research trends on unmanned aerial vehicles (UAVs). 11(8):400. Number: 8 Publisher: Multidisciplinary Digital Publishing Institute.

3. Giulio Avanzini, Emanuele L. de Angelis, Daniele Fattizzo, and Fabrizio Giulietti. Autorotation design and simulation for a small-scale helicopter. In *48rd European Rotorcraft Forum, ERF 2022*.

4. Ioannis A. Raptis and Kimon P. Valavanis. *Linear and Nonlinear Control of Unmanned Rotorcraft*. Springer Dordrecht, 2010.

5. Hanafy M. Omar. Hardware-in-the-loop simulation of time-delayed anti-swing controller for quadrotor with suspended load. 12(3):1706. Number: 3 Publisher: Multidisciplinary Digital Publishing Institute.

6. Igor Henrique Beloti Pizetta, Alexandre Santos Brandão, and Mário Sarcinelli-Filho. A hardware-in-the-loop platform for rotary-wing unmanned aerial vehicles. 84(1):725–743.

7. Muhsin Hancer, Rahman Bitirgen, and Ismail Bayezit. Designing 3-DOF hardware-in-the-loop test platform controlling multirotor vehicles. 51(4):119–124.

8. F. Prochazka, S. Krüger, G. Stomberg, and M. Bauer. Development of a hardware-in-the-loop demonstrator for the validation of fault-tolerant control methods for a hybrid UAV. 12(3):549–558.

9. Yaqub Aris Prabowo, Bambang Riyanto Trilaksono, and Fadjar Rahino Triputra. Hardware in-the-loop simulation for visual servoing of fixed wing UAV. In *2015 International Conference on Electrical Engineering and Informatics (ICEEI)*, pages 247–252. ISSN: 2155-6830.

10. Saran Khaliq, Shahzeb Ahsan, and Muhammad Nisar. *Multi-Platform Hardware In The Loop (HIL) Simulation for Decentralized Swarm Communication Using ROS and GAZEBO*. Pages: 315.

11. Jingxuan Sun, Boyang Li, Chih-Yung Wen, and Chih-Keng Chen. Design and implementation of a real-time hardware-in-the-loop testing platform for a dual-rotor tail-sitter unmanned aerial vehicle. 56:1–15.

12. Li Yu, Guang He, Shulong Zhao, Xiangke Wang, and Lincheng Shen. Design and implementation of a hardware-in-the-loop simulation system for a tilt trirotor UAV. 2020:e4305742. Publisher: Hindawi.

13. Sepehr P. Khaligh, Alejandro Martínez, Farbod Fahimi, and Charles Robert Koch. A HIL testbed for small unmanned helicopter's initial controller gain tuning. In *2013 International Conference on Unmanned Aircraft Systems (ICUAS)*, pages 383–391.

14. Guowei Cai, Ben Chen, Tong Lee, and Miaobo Dong. Design and implementation of a hardware-in-the-loop simulation system for small-scale UAV helicopters. 19:1057–1066.

15. Praney Dubey, Vineet Singh, and Mohit Mangal. Design and comparison of control schemes for UAV autopilot. 45(1):103–108.

16. A.S. Holtsov, R.M. Farhadi, V.I. Kortunov, and A. Mohammadi. Comparison of the UAV adaptive control with the robust control based on mu-synthesis. In *2016 4th International Conference on Methods and Systems of Navigation and Motion Control (MSNMC)*, pages 18–21.

17. Rui Ming, Rui Jiang, Haibo Luo, Taotao Lai, Ente Guo, and Zhiyan Zhou. Comparative analysis of different UAV swarm control methods on unmanned farms. 13(10):2499. Number: 10 Publisher: Multidisciplinary Digital Publishing Institute.

18. Safeena Qadir, Shahida Khatoon, and Mohammad Shahid. Comparison of conventional, modern and intelligent control techniques on uav control. In *2023 International Conference on Power, Instrumentation, Energy and Control (PIECON)*, pages 1–6.

19. P. D. Talbot, B. E. Tinling, W. A. Decker, and R. T. N. Chen. A mathematical model of a single main rotor helicopter for piloted simulation. Technical Report NAS 1.15:84281, September 1982. NTRS Author Affiliations: NASA Ames Research Center NTRS Document ID: 19830001781 NTRS Research Center: Legacy CDMS (CDMS).

20. Giulia Bertolani, A. D. Ryals, L. Pollini, and F. Giulietti. L1 adaptive speed control for a helicopter. In *48rd European Rotorcraft Forum, ERF 2022*. Associazione Italiana di Aeronautica e Astronautica (AIDAA), 2022.

21. U.S. Government Printing Office, U.S. Standard Atmosphere, NOAA-S/T 76-1562, Washington, D.C., 1976, 1–241.

22. R.K. Heffley and M. A. Mnich. Minimum complexity helicopter simulation math model, April 1988. Ames Reasearch Center, Moffett, Field, California.

23. J. Gordon. Leishman. *Principles of helicopter aerodynamics*. Cambridge aerospace series 12. Cambridge University Press, Cambridge, 2000.

24. D. A. Peters and N. HaQuang. Dynamic inflow for practical applications. *Journal of the American Helicopter Society*, 33(4):64–68, 1988.

25. G. Szafranski and C. Roman. Different approaches of pid control uav type quadrotor. In *The international micro air vehicles conference*, pages 70–75, 2011.

26. Giulia Bertolani, Andrea Dan Ryals, Emanuele Luigi de Angelis, and Fabrizio Giulietti. Hierarchical dual-loop speed control for a helicopter. In *49th European Rotorcraft Forum, ERF 2023*, September.

27. O. Halbe and M. Hajek. Robust helicopter sliding mode control for enhanced handling and trajectory following. *Journal of Guidance, Control, and Dynamics*, 43(10), 2020.

28. Matlab/Simulink. Px4 autopilot in hardware-in-the-loop (hitl) simulation with uav dynamics in simulink. https://it.mathworks.com/help/supportpkg/px4/ref/hitl-simulink-plant-example.html.

29. United States Army, Aviation and Missile Command., Aeronautical design standard, performance specification and handling qualities requirements for military rotorcraft, March 2000.

Table 1. UAV helicopter relevant parameters

Parameter	Symbol	Value	Units
UAV DATA			
Mass	m	4.8	kg
Center of gravity stationline	STA_{CG}	0.34	m
Center of gravity buttline	BL_H	0	m
Center of gravity waterline	WL_H	0.174	m
Moment of inertia	I_x, I_y, I_z	0.0465, 0.2971, 0.2567	kg m^2
Inertia products	I_{xy}, I_{yz}, I_{xz}	0.0079, 0.0033, 0.0006	kg m^2
MAIN ROTOR (MR)			
Number of blades	N_b	2	-
Radius	R_{MR}	0.79	m
Chord	c_{MR}	0.06	m
Rotational speed	Ω_{MR}	1995.3	rpm
Hinge offset	ε	0.0314	m
Flapping spring constant	K_β	162.69	N m/rad
Tangent of δ_3	K_1	0	-
Blade twist	θ_{tMR}	0	rad
Precone angle	a_{0MR}	0	rad
Solidity	σ_{MR}	0.0479	-
Lift curve slope	a_{TR}	2*π	1/rad
Blade inertia moment	I_β	0.0344	kg m^2
MR hub stationline	STA_H	0.3305	m
MR hub buttline	BL_H	0	m
MR hub waterline	WL_H	0.35	m
TAIL ROTOR (TR)			
Number of blades	N_b	2	-
Radius	R_{TR}	0.115	m
Chord	c_{TR}	0.031	m
Rotational speed	Ω_{TR}	9976	rpm
Tangent of δ_3	K_{1TR}	0	-
Blade twist	θ_{tMR}	0	rad
Solidity	σ_{TR}	0.1716	-
Lift curve slope	a_{TR}	2*π	1/rad
Blade inertia moment	I_β	0.00002665	kg m^2
TR hub stationline	STA_{TR}	1.385	m
TR hub buttline	BL_{TR}	0.052	m
TR hub waterline	WL_{TR}	0.205	m
FUSELAGE (FUS)			
Fus. aerodynamic ref. point stationline	STA_{FUS}	0	m
Fus. aerodynamic ref. point buttline	BL_{FUS}	0	m
Fus. aerodynamic ref. point waterline	WL_{FUS}	0	m
Frontal area	S_{front}	0.02042	m^2
Lateral area	S_{lat}	0.0633	m^2
Top area	S_{top}	0.09739	m^2